

## Seeing topological order

E. Alba,<sup>1</sup> X. Fernandez-Gonzalvo,<sup>1</sup> J. Mur-Petit,<sup>1</sup> J. K. Pachos,<sup>2</sup> and J. J. Garcia-Ripoll<sup>1</sup>

<sup>1</sup>*Instituto de Física Fundamental, IFF-CSIC, Calle Serrano 113b, Madrid 28006, Spain*

<sup>2</sup>*School of Physics and Astronomy, University of Leeds, Leeds, LS2 9JT, United Kingdom*

(Dated: March 29, 2025)

In this work we provide a general methodology to directly measure topological order in cold atom systems. As an application we propose the realisation of a characteristic topological model, introduced by Haldane, using optical lattices loaded with fermionic atoms in two internal states. We demonstrate that time-of-flight measurements directly reveal the topological order of the system in the form of momentum space skyrmions.

PACS numbers: 67.85.-d,03.65.Vf

Different phases of matter can be distinguished by their symmetries. This information is usually captured by locally measurable order parameters that summarize the essential properties of the phase. Topological insulators are materials with symmetries that depend on the topology of the energy eigenstates of the system [1]. These materials are of interest because they give rise to robust spin transport effects with potential applications ranging from sensitive detectors to quantum computation [2, 3]. However, direct observation and measurement of topological order has been up to now impossible due to its non-local character. Instead, experiments have relied so far on indirect manifestations of this order, such as edge states and the quantization of conductivity.

One common mechanism for the appearance of topological order is based on the topology of the eigenstate manifolds. Consider a real-space lattice whose unit cell has  $d$  quantum degrees of freedom —position of the particle, spin, etc—. Its energy band description,  $E_m(\mathbf{k})$ , has  $d$  eigenstates,  $\psi_{m=1\dots d}(\mathbf{k})$ , per value of momentum  $\mathbf{k} = (k_x, k_y)$  in the Brillouin zone,  $\mathcal{B}$ . Different configurations of the vector fields,  $\psi_m$ , can be characterised by topological invariants such as the Chern number of each band [3],

$$\nu_m = \frac{1}{2\pi} \int_{\mathcal{B}} \nabla_{\mathbf{k}} \times \mathbf{v}_m d^2\mathbf{k}, \quad \mathbf{v}_m = i\langle \psi_m | \nabla_{\mathbf{k}} \psi_m \rangle. \quad (1)$$

In the case of the quantum Hall effect, the energy bands are separated from each other and the material becomes an insulator for appropriate Fermi energies,  $E_F$ . In a real setup, with finite boundaries, the sample can have a quantized non-zero conductivity given by the topological invariant  $\sigma_{xy}^m = e^2/h \sum_{E_m < E_F} \nu_m$ , which is a signature itself of topological order. The transport is then supported by “edge” states that are localized on the boundary of the material, with interesting properties, such as spin polarization or chirality, insulation from noise and resilience to perturbations [3].

There are two essential routes towards topological order in momentum space, depending on how we realize the  $d$  quantum degrees of freedom mentioned above. One is to start from charge carriers with intrinsic angular mo-

mentum and a spin-orbit coupling. This is the case of the Kane model [1] or in models with semiconductor structures [4]. A different approach is exemplified by the Haldane model [5]. This model is built on a honeycomb lattice where the unit cell has two sites and the parity symmetry is broken using a spatially modulated magnetic field. Here we propose a method to realize a generalization of the Haldane model using optical lattice technology. Our idea is to employ two atomic hyperfine levels (pseudospin) to distinguish between the sites of the unit cell. This enables us to directly extract the Chern number from the spin textures in time-of-flight images [6] and thus demonstrate the topological order of the system. This procedure can be directly translated to other proposals for quantum simulation of topological order in optical lattices, thanks to the fact that many of those proposals already use internal degrees of freedom of the atoms to encode the order [7–16].

Let us consider a honeycomb lattice constructed out of two triangular sublattices, A and B, as shown in Fig. 1a. Each of the sublattices hosts fermionic alkali atoms in a different internal state,  $|a\rangle$  and  $|b\rangle$ . The model will be parameterised by three couplings: the hopping amplitudes inside the same species lattice,  $t_a$  and  $t_b$ , the energy difference between A and B sublattices,  $\varepsilon$ , and the coupling between sublattices,  $t_{jk}$ . We assume that the lattice is deep enough, so that  $t_{a,b}$  and  $\varepsilon$  are small perturbations to the honeycomb lattice hopping,  $t_{jk}$ , which can be induced by a Raman laser and controlled at will. In the presence only of the hopping  $t_{jk}$  the energy spectrum comprises of two energy bands that meet at two points (“Dirac points”). At half filling the low energy physics of the system is dominated by the energy dispersion around these points, which is linear, giving rise to “Dirac cones” [17]. Due to the presence of  $t_{a,b}$  and  $\varepsilon$ , the effective Dirac fermions acquire a mass that depends weakly on momentum. The position of the Dirac points on the mass landscape determines whether the model is topologically ordered or not. The cold atoms simulation provides the knobs to interpolate between these two regimes. Raman transitions[18] give the ability to attach

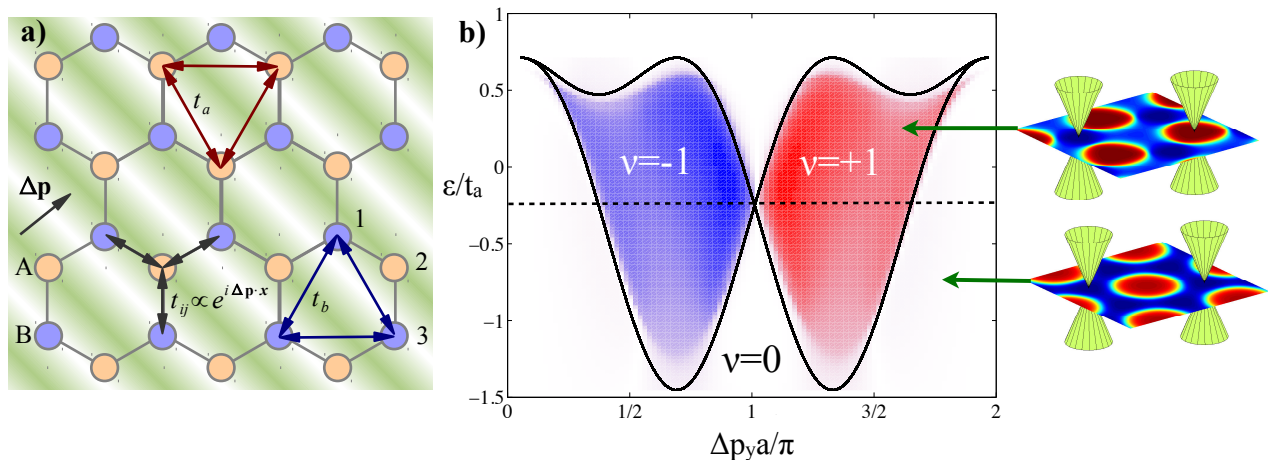


FIG. 1: Haldane-type model. (a) Two triangular optical lattices (A and B) are Raman coupled by a laser that makes an atom switch sublattice ( $A \leftrightarrow B$ ). This allows for both next-nearest neighbor hoppings,  $t_{a,b}$ , and a complex nearest neighbor hopping,  $t_{jk}$ , whose phase depends on the momentum imparted by the Raman laser,  $\Delta \mathbf{p}$ . (b) Phase diagram of the zero-energy ground states, as a function of the energy imbalance between lattices,  $\varepsilon/t_a$ , and the momentum imparted by the laser,  $\Delta \mathbf{p} = (0, \Delta p_y)$ . We plot the exact phase boundary in the thermodynamic limit (black solid line), together with a color graded simulation of the Chern number for a finite lattice with 1000 sites. The diagrams on the right hand side show how the Dirac points are displaced on the distribution of Bloch vectors  $S_z(\mathbf{k})$  induced by the Hamiltonian (blue negative, red positive).

a phase to the hopping

$$t_{jk} \sim t \exp(i\phi_{jk}), \quad \phi_{jk} = \Delta \mathbf{p} \cdot (\mathbf{x}_j + \mathbf{x}_k)/2. \quad (2)$$

This corresponds to a momentum boost in the Brillouin zone,  $\Delta \mathbf{p}$ , which displaces the energy bands created by the Raman hopping,  $t$ , relative to the other contributions,  $t_{a,b}$  and  $\varepsilon$ . While the total flux over each hexagonal plaquette is zero, the bipartite nature of the lattice allows the phases  $\phi_{jk}$  to have a non-trivial effect: along the path  $1 \rightarrow 2 \rightarrow 3 \rightarrow 1$ , depicted in Fig. 1a the local effective magnetic flux, given by  $\phi_{12} + \phi_{23}$ , is non-zero.

The single-particle model with all the previous ingredients can be well approximated by a family of momentum space Hamiltonians written as [3]

$$\mathcal{H}(\mathbf{k}) \sim -E \mathbf{S}(\mathbf{k}) \cdot \boldsymbol{\sigma}. \quad (3)$$

Here,  $E$  is an energy scale,  $\boldsymbol{\sigma} = (\sigma^x, \sigma^y, \sigma^z)$  are the Pauli matrices and the unit vector  $\mathbf{S}$  is the pseudospin in the space of internal states of the atom,  $|a\rangle, |b\rangle$ . All topological properties of the model can be obtained from studying the momentum configuration of the vector field  $\mathbf{S}$ . In particular, the eigenstates of the lowest energy band are pure states determined by the Bloch vector  $\mathbf{S}$  and give this band a total Chern number

$$\nu = \frac{1}{4\pi} \int_{\mathcal{B}} \mathbf{S} \cdot (\partial_{k_x} \mathbf{S} \times \partial_{k_y} \mathbf{S}) d^2 k. \quad (4)$$

In our setup, the distribution  $\mathbf{S}(\mathbf{k}) = \langle \boldsymbol{\sigma} \rangle$  can be experimentally determined from the time-of-flight images that appear when the atoms are released from the optical trap [6]. The idea is to fill the lattice with enough atoms

to cover the lowest energy band. The experiment may begin with a Mott state in which only the A sublattice is filled, and adiabatically progress towards larger values of  $t_a$ ,  $t$  and  $\varepsilon$ . Once the approximate ground state is prepared, switching off the trap in adequate timescales [6] transforms the atom cloud into the momentum distributions of its density,  $n_{a,b}(\mathbf{k})$ , giving direct access to  $S_z(\mathbf{k}) = \frac{1}{2}[n_a(\mathbf{k}) - n_b(\mathbf{k})]$ . By performing in-flight rotations of the atomic states we can also obtain  $S_x$  and  $S_y$ , thus reconstructing the whole vector field and the associated topological invariant,  $\nu$ .

Note that in practice experiments will have to “pixelize” the time of flight images, counting the number of atoms on each “square” of the effective Brillouin zone and estimating the averages of  $S_x$ ,  $S_y$  or  $S_z$ . After many repetitions this method will provide a discrete distribution of normalized vectors  $\{\mathbf{S}_m\}_{m=1}^{L \times L}$ , on a lattice evenly sampled over momentum space. We suggest grouping the pixels, partitioning the experimental image into sets of triangles,  $T = \{\mathbf{S}_{j_T}, \mathbf{S}_{k_T}, \mathbf{S}_{l_T}\}$ . The momentum integral in (4) restricted to the any such triangle is half the solid angle covered by the spins that sit on its corners. Therefore, we may construct a “discretized” version of the Chern number,  $\nu_D \simeq \sum_T \frac{1}{8\pi} \mathbf{S}_{j_T} \cdot \mathbf{S}_{k_T} \times \mathbf{S}_{l_T}$ , which for all purposes will be sufficiently close to  $\nu$ , while retaining its stability and robustness against local perturbations.

Experimentally, the setup could be realized by combining ideas for spin-dependent potentials [19, 20], with recent techniques for creating dipole traps using microscope objectives [21]. More precisely, we suggest projecting two triangular lattice patterns on a two-dimensional sheet of light that traps the fermionic atoms. An electro-

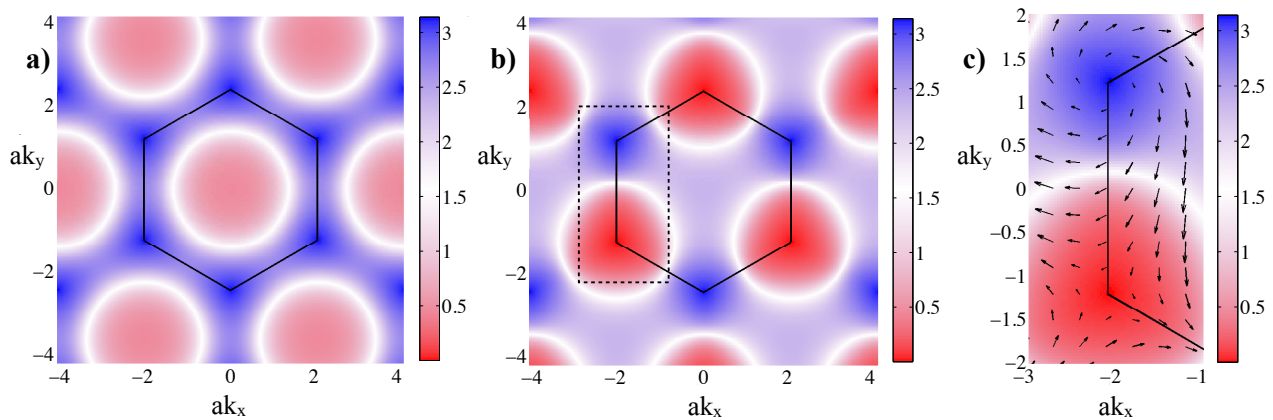


FIG. 2: Spin textures of the Haldane model. These textures are interpreted as a mapping from momentum space,  $(k_x, k_y)$ , on to the Bloch sphere,  $\mathbf{S} = \langle \boldsymbol{\sigma} \rangle \propto (\cos \phi \sin \theta, \sin \phi \sin \theta, \cos \theta)$ . In colors we plot the polar angle  $\theta(\mathbf{k})$ , for Chern numbers (a)  $\nu = 0$  and (b)  $\nu = +1$ . All phases share the same distribution  $\phi(\mathbf{k})$ , which is represented in (c) as the azimuthal component of the spin,  $(S_x, S_y)$ . (a) For  $\varepsilon = 0$  and  $\Delta \mathbf{p} = (0, 0)$  we have two merons sitting on both Dirac cones, at the vertices of the depicted hexagon. Both merons sit on the same pole,  $S_z < 0$ , and have opposite topological charges. (b) At  $\Delta \mathbf{p} = (0, 4\pi/3\sqrt{3})$ , the effective masses on the cones have different signs, so the two merons together form a skyrmion. (c) Detail of (b) around the Dirac points (dashed rectangle) that shows how the skyrmion covers everything from the north (red) to the south pole (blue).

optic phase modulator controls the relative displacement of the lattices [22], while imposing that each of them be a particular combination of left and right circularly polarized light, as in Refs. [19, 20]. The result is two hyperfine ground states of the same fermionic species confined on the two triangular sublattices of the honeycomb pattern.

We have theoretically studied our model using both the ideal, thermodynamic limit distribution  $\mathbf{S}(\mathbf{k})$ , as well as realistic finite-size lattices with imperfections. Since the tunneling amplitudes and interaction energies will be small compared to the interband separation [23], we can use the single band tight-binding model

$$H = \sum_{(j,k)} (t_{jk} b_j^\dagger a_k + t_{jk}^* a_k^\dagger b_j) + \sum_j \varepsilon (a_j^\dagger a_j - b_j^\dagger b_j) + \sum_{\langle\langle j,k \rangle\rangle} t_a a_j^\dagger a_k + \sum_{\langle\langle j,k \rangle\rangle} t_b b_j^\dagger b_k. \quad (5)$$

The momentum space Hamiltonian associated to this model has the form

$$\mathcal{H}(\mathbf{k}) = \begin{pmatrix} \varepsilon/2 + t_a g(\mathbf{k}) & t f(\mathbf{k} - \Delta \mathbf{p}) \\ t f(\mathbf{k} - \Delta \mathbf{p})^* & -\varepsilon/2 + t_b g(\mathbf{k}) \end{pmatrix} \quad (6)$$

with the complex functions  $f(\mathbf{k}) = \sum_{n=0,1,2} e^{i\mathbf{k} \cdot \mathbf{v}_n a}$ , and  $g(\mathbf{k}) = \sum_{n=3,4,5} 2 \cos(\mathbf{k} \cdot \mathbf{v}_n a)$ , the lattice spacing  $a$ , and a set of displacements  $\mathbf{v}_0 = (-1, 0)$ ,  $\mathbf{v}_1 = \frac{1}{2}(1, \sqrt{3})$ ,  $\mathbf{v}_2 = \frac{1}{2}(1, -\sqrt{3})$ ,  $\mathbf{v}_3 = (0, \sqrt{3})$ ,  $\mathbf{v}_4 = \frac{1}{2}(3, \sqrt{3})$  and  $\mathbf{v}_5 = \frac{1}{2}(3, -\sqrt{3})$ . As explained before, for each momentum eigenstate we can identify the internal state of the atoms with a vector on the Bloch sphere,  $\mathbf{S}(\mathbf{k}) = (t \text{Re} f(\mathbf{k} - \Delta \mathbf{p}), t \text{Im} f(\mathbf{k} - \Delta \mathbf{p}), \varepsilon + \frac{1}{2}(t_a - t_b)g(\mathbf{k}))$ .

Fig. 1b summarizes the three different phases that can be accessed by means of the effective magnetic flux,  $\Delta \mathbf{p} =$

$(0, \Delta p_y)$ , and the imbalance between lattices,  $\varepsilon/t_a$ . First of all we find a trivial region,  $\nu = 0$ , which is topologically equivalent to graphene with a mass term. As shown in Fig. 2a, when we interpret the associated spin texture as a map onto the Bloch sphere, both cones have the same effective Dirac mass and point to the same pole,  $S_z > 0$ . Two merons are formed with opposite charges, covering the same polar cap in opposite senses, that is  $\nu = \pm(\frac{1}{2} - \frac{1}{2}) = 0$ . When we cross over the solid black line in Fig. 1b, the lattice undergoes a quantum phase transition into a topologically non-trivial phase. Now the cones on inequivalent Dirac points are positioned at opposite poles of the Bloch sphere, and the two merons form a single skyrmion that covers the whole sphere [24]. Thus, in this new phase the total Chern number is  $\nu = \pm(\frac{1}{2} + \frac{1}{2}) = \pm 1$ .

In order to study realistic experimental scenarios we have simulated Hamiltonian (5) on a finite lattice from 500 up to 20000 sites, including an additional harmonic confinement term,  $\frac{1}{2}m\omega^2 x_i^2$ . We found that the topological phases are robust under various conditions, which include (i) use of small finite lattices (ii) coarse grain measurements of the spin texture, (iii) inhomogeneous potentials superimposed on top of the lattice, and (iv) errors in the exact values of the chemical potential, number of atoms or in the presence of finite temperature.

In our plots we report simulations with hoppings  $t/\hbar = 1$  kHz and  $t_a/t = 0.2$ , where  $r = m\omega^2 a^2/2t$  is the control parameter to study the influence of the harmonic confinement [Fig. 3]. Typical values for a lattice with  $a \sim 400$ nm range from  $r = 10^{-3}$  ( $^6\text{Li}$  in a trap with  $\omega/2\pi = 60$  Hz) to  $r = 0.02$  ( $^{40}\text{K}$  in a trap with  $\omega/2\pi = 100$  Hz). The main message of our simulations is the stability of the discretized version of the Chern number and of our topo-

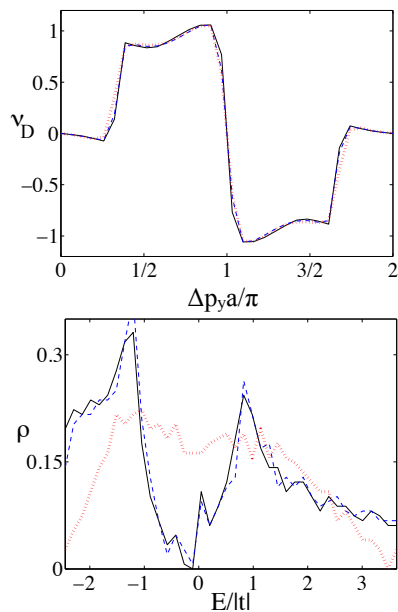


FIG. 3: Simulation of the measurement procedure with 1000 atoms in a uniform lattice (black, solid) or with a confining harmonic potential which is weak  $r = m\omega^2 a^2/2t = 10^{-3}$  (blue, dashed) or stronger  $r = 0.02$  (red, dotted). (a) Phase diagram along the dashed black line in Fig. 1(b), plotting the discretized Chern number,  $\nu_D$ , versus the Haldane model parameter. (b) Density of states in energy space. Notice that while having a confining potential severely affects the density of states,  $\rho$ , the estimate of the topological invariant,  $\nu$ , is very stable.

logical phases. First of all, the results are very insensitive to the number of atoms, as already for  $20 \times 20$  sites the vector fields look very similar to those of Fig. 2. Furthermore, the approximate Chern number shown in Fig. 3a, is robust against inhomogeneities, while the density of states and the eigenenergies are not. As show in Fig. 3b, for a confining trap with  $r = 0.02$  the Dirac cones are no longer evident, while the Chern number is close to  $\pm 1$  for the topological phases. Finally, the roughness of the pixelization in the time-of-flight images is not a problem: in our work we report results that use  $400 = 20 \times 20$  pixels on a Brillouin zone, but the phase diagram is very similar for even coarser grainings.

Summing up, in this work we presented a robust method to detect topological order in momentum space using ultracold atoms in various internal states and time-of-flight images. As a very relevant application we have introduced an experimental proposal to realize the Haldane model [5]. This model bears topological order and other interesting features such as edge states. We have demonstrated that the identification of the topological phases can be performed faithfully even for small lattices under severe perturbations. We believe our proposal is thus advantageous with respect to other indirect detection schemes, such as edge transport, eigenstate preparation [10] or local approximations of the density

of states [25]. Moreover, the implementation of our ideas would represent the first direct visualization of non-local topological order in a physical system, and can be generalized to other quantum simulations of topological order in optical lattices [7–16].

This work has been funded by Spanish MICINN Project FIS2009-10061, FPU grant No.AP 2009-1761, CAM research consortium QITEMAD S2009-ESP-1594, a Marie Curie Intra European Fellowship, JAE-INT-1072 CSIC scholarship and the Royal Society.

- 
- [1] C. L. Kane and E. J. Mele, Phys. Rev. Lett. **95**, 226801 (2005).
  - [2] C. Nayak, S. H. Simon, A. Stern, M. Freedman, and S. Das Sarma, Rev. Mod. Phys. **80**, 1083 (2008).
  - [3] M. Z. Hasan and C. L. Kane, Rev. Mod. Phys. **82**, 3045 (2010).
  - [4] B. A. Bernevig and S.-C. Zhang, Phys. Rev. Lett. **96**, 106802 (2006).
  - [5] F. D. M. Haldane, Phys. Rev. Lett. **61**, 2015 (1988).
  - [6] M. Köhl, H. Moritz, T. Stöferle, K. Günter, and T. Esslinger, Phys. Rev. Lett. **94**, 080403 (2005).
  - [7] A. Bermudez, N. Goldman, A. Kubasiak, M. Lewenstein, and M. A. Martin-Delgado, New J. Phys **12**, 033041 (2010).
  - [8] A. Kubasiak, P. Massignan, and M. Lewenstein, Europhysics Letters **92**, 46004 (2010).
  - [9] A. Bermudez, L. Mazza, M. Rizzi, N. Goldman, M. Lewenstein, and M. A. Martin-Delgado, Phys. Rev. Lett. **105**, 190404 (2010).
  - [10] N. Goldman, I. Satija, P. Nikolic, A. Bermudez, M. A. Martin-Delgado, M. Lewenstein, and I. B. Spielman, Phys. Rev. Lett. **105**, 255302 (2010).
  - [11] T. Pereg-Barnea and G. Refael, arXiv:1011.5243.
  - [12] B. Béri and N. R. Cooper, arXiv:1105.1252.
  - [13] L. Mazza, A. Bermudez, N. Goldman, M. Rizzi, M. A. Martin-Delgado, and M. Lewenstein, arXiv:1105.0932.
  - [14] T. D. Stanescu, V. Galitski, and S. Das Sarma, Phys. Rev. A **82**, 013608 (2010).
  - [15] J. D. Sau, R. Sensarma, S. Powell, I. B. Spielman, and S. Das Sarma, Phys. Rev. B **83**, 140510 (2011).
  - [16] K. Sun, Z. Gu, H. Katsura, and S. Das Sarma, arXiv:1012.5864.
  - [17] P. R. Wallace, Physical Review **71**, 622 (1947).
  - [18] D. Jaksch and P. Zoller, New J. Phys **5**, 56 (2003).
  - [19] O. Mandel, M. Greiner, A. Widera, T. Rom, T. W. Hänsch, and I. Bloch, Nature **425**, 937 (2003).
  - [20] D. Jaksch, C. Bruder, J. I. Cirac, C. W. Gardiner, and P. Zoller, Phys. Rev. Lett. **81**, 3108 (1998).
  - [21] W. S. Bakr, J. I. Gillen, A. Peng, S. Fölling, and M. Greiner, Nature **462**, 74 (2009).
  - [22] K.-A. B. Soderberg, N. Gemelke, and C. Chin, New J. Phys **11**, 055022 (2009).
  - [23] M. Eckholt and J. Garcia-Ripoll, New J. Phys **11** (2009).
  - [24] G. Volovik, *The Universe in a Helium Droplet* (Oxford University Press, 2003), chap. 11.
  - [25] S.-L. Zhu, B. Wang, and L.-M. Duan, Phys. Rev. Lett. **98**, 260402 (2007).